1992

Main Geometric Characteristics of the Twin Screw Compressor

L. Zhang
Wuxi Compressor Works; P. R. China

J. F. Hamilton
Purdue University

MAIN GEOMETRIC CHARACTERISTICS OF THE TWIN SCREW COMPRESSOR

by

Liankang Zhang
Wuxi Compressor Works
CHINA
and
James F. Hamilton
Ray W. Herrick Laboratories, School of Mechanical Engineering
Purdue University, West Lafayette, IN 47907-1077, USA

ABSTRACT

The geometric characteristics of twin screw compressors greatly effect their performance and efficiency. In the use of computer modeling and simulation methods for the prediction of twin screw compressor performance, a basic problem is the analysis and calculation of the geometry characteristics. This paper presents the calculation of the main geometry characteristics, such as the compression volume curve, the sealing line length, the flute area, and the wrap angle factors, and the blow hole area.

NOMENCLATURE

xyz, XYZ :	body fixed and inertial reference frames for the male and female rotors
r :	pitch radius for the male and female rotors
R :	radius of the lobe for the male and female rotors
i :	transmission ratio between the rotors
m :	teeth number of the rotors
ϕ_1 :	turning angle for the male rotor
v :	volume of the rotor working space
h :	screw characteristics for the male and female rotors
T :	rotor lead for the male and female rotors
β_{01} :	angle at the point where the housing cross
τ_{1z} :	wrap angle of the male rotor
p :	pressure
l_r :	rotor length
v_d :	discharge volume
η_v :	volumetric efficiency
f_0 :	flute area of the rotor
c_n :	flute area factor
c_ϕ :	wrap angle factor
n :	rotation speed
D_1 :	diameter of the male rotor
Δv_{01} :	occupied volume of the male rotor by the female rotor
v_0 :	flute volume of the rotor
λ :	parameter variable
ψ :	position variable
k :	$= T/2\pi$
1, 2 :	scripts referring to the male and female respectively
s, d :	scripts referring to the suction and discharge

1. INTRODUCTION

The twin screw compressor, as a rotary, positive displacement compressor, has gained an important position in the gas compressor industry. This position has led to the consideration of different screw profiles and the development of modern machine processes for their production [1,2]. The use of computer simulation and modeling to predict the performance and efficiency of these different profiles has been used to speed the development of improved profiles.

The geometric characteristics are complicated to model in the computer simulation of twin screw compressors. This paper presents the determination of certain important geometric characteristics which strongly affect the performance and efficiency of the compressor:

a) compression volume curve
b) sealing line length
c) flute area factor
d) wrap angle factor
e) blow hole area

2. PROFILE CONSTRUCTION

A pair of rotor profiles are utilized as an example in the determination of the listed geometric characteristics. The following table presents the male and female profiles used. The profiles are also shown in Figure 1. Two separate rotor fixed coordinate frames x_1, y_1 and x_2, y_2 are used in describing the mating profiles.

Female	Profiles	Profiles mating with
a_2b_2	pitch circle of r_2	a_1b_1
b_2c_2	arc	b_1c_1
c_2d_2	straight line	c_1d_1
d_2e_2	arc	d_1e_1
e_2f_2	epicycloid curve	e_1f_1
f_2g_2	straight line	f_1g_1
Male	**Profiles**	**Profiles mating with**
a_1b_1	pitch circle of r_1	a_2b_2
b_1c_1	envelop curve	b_2c_2
c_1d_1	envelop curve	c_2d_2
d_1e_1	arc	d_2e_2
e_1f_1	epicycloid curve	e_2f_2
f_1g_1	epicycloid curve	f_2g_2

Table 1 Example Twin Screw Mating Profiles

3. COMPRESSION VOLUME CURVE

The compression volume curve can be obtained by integrating the swept area along the length of the rotor, or by employing the principle of virtual work [3]. A third method is presented here which computes the compression volume curve of twin screw compressors by using the profile functions directly.

3.1 Principle of Computation

When an area is enclosed by two lines (in parametric form),

$$L_1 = \begin{cases} x_1 = x_1(t) \\ y_1 = y_1(t) \end{cases} \qquad L_2 = \begin{cases} x_2 = x_2(t) \\ y_2 = y_2(t) \end{cases}$$

the value of the area can be calculated by integrating between the lines. The area shown in Figure 2 Sabcd will be

$$S_{abcd} = \frac{1}{2} \oint (x\,dy - y\,dx)$$

$$= \frac{1}{2} \int_{t_{1a}}^{t_{1c}} (\dot{y}_1 x_1 - \dot{x}_1 y_1)\,dt_1 + \frac{1}{2} \int_{t_{2c}}^{t_{2a}} (\dot{y}_2 x_2 - \dot{x}_2 y_2)\,dt_2$$

where t_{1a} and t_{1c} are the values of t_1 at point a and point c, and t_{2c} and t_{2a} are the values of t_2 at point c and point a. It is generally simple to calculate the compression area in the grooves of the rotors by employing this principle.

3.2 Profile Functions of the Rotors

Before computing the volume curve, it is necessary to establish the profile functions for the male and female rotors, which are based on the rotor fixed frames shown in Figure 3. For example, the functions of profile segment de are for the male rotor

$$\begin{cases} x_1 = r_1 + R\cos t \\ y_1 = -R\sin t \end{cases} ; \quad t_1 \le t \le t_2$$

and for the female rotor

$$\begin{cases} x_2 = r_2 - R\cos t \\ y_2 = -R\sin t \end{cases} ; \quad t_1 \le t \le t_2$$

where t_1 and t_2 are the values of the parameter at the points e and d. The integration process must be based on the same coordinate frame and therefore the profile functions for the female rotor are transfered into the coordinate frame of the male rotor. The transfer relation is as follows,

$$\begin{cases} x_1 = -x_2\cos(k\varphi_1) + y_2\sin(k\varphi_1) + a\cos\varphi_1 \\ y_1 = x_2\sin(k\varphi_1) + y_2\cos(k\varphi_1) - a\sin\varphi_1 \end{cases}$$

and the function of profile segment d_2e_2 becomes

$$\begin{cases} x_1 = -r_2\cos(k\varphi_1) + R\cos(t + k\varphi_1) + a\cos\varphi_1 \\ y_1 = r_2\sin(k\varphi_1) - R\sin(t + k\varphi_1) - a\cos\varphi_1 \end{cases}$$

Note that there are two teeth taking part in the mating process for the rotor, the leading lobe and the trailing lobe, and that the transfer relations used for them are different.

The transfer relations for the male and female rotors are as follows:

For the male rotor

$$\begin{vmatrix} \cos\left(\frac{2\pi}{m_2}\right) & -\sin\left(\frac{2\pi}{m_2}\right) \\ \sin\left(\frac{2\pi}{m_2}\right) & \cos\left(\frac{2\pi}{m_2}\right) \end{vmatrix}$$

and for the female rotor

$$\begin{vmatrix} \cos\left(\frac{2\pi}{m_1}\right) & -\sin\left(\frac{2\pi}{m_1}\right) \\ \sin\left(\frac{2\pi}{m_1}\right) & \cos\left(\frac{2\pi}{m_1}\right) \end{vmatrix}$$

3.3 Calculation of the Compression Area

When the lobe tip point a_2 of the female profile reaches the point H, as in Figure 3, the compression process begins. At this moment the turning angle of the male rotor is φ_{10} and the groove areas f_{01} and f_{02} for the male and female rotor are at their maximum values.

At a different moment, shown in Figure 4, there is only one point mating between two rotors and the shaded area is the uncompressed area of the grooves. This area S can be computed using the principle stated in 3.1,

$$S = \oint (L_1 + L_2 + L_3 + L_4)$$

where

$$L_1 = f_2 f_1 a_1 b_1 c_1 d_1 e_1' \qquad L_3 = e_1' H$$

$$L_3 = H g_2 \qquad L_4 = g_2 f_2 e_2 d_2 c_2 b_2 a_2 f_2'$$

Lines L_1 and L_4 consist of several pieces of profiles for the male and female rotors. Profile segment $a_1 b_1$ is an example to illustrate the use of this method. This segment has a circular shape with a profile given by

$$\begin{cases} x_1 = r_1 \cos t \\ y_1 = r_1 \sin t \end{cases} ; \quad t_{a_1} \le t \le t_{b_1}$$

and t_{a1} and t_{b1} are parametric values. The time derivatives are

$$\begin{cases} \dot{x}_1 = -r_1 \sin t \\ \dot{y}_1 = r_1 \cos t \end{cases}$$

The integration function is

$$f(t) = \frac{1}{2}(\dot{y}_1 x_1 - \dot{x}_1 y_1) = \frac{1}{2} r_1^2$$

It is clear that as the parameter t changes from t_{a1} to t_{b1}, the integration of the function will be

$$\int_{t_{a_1}}^{t_{b_1}} f(t)\,dt = F(t_{b_1}) - F(t_{a_1}) = \frac{1}{2} r_1^2 \cdot (t_{b_1} - t_{a_1})$$

that is, the area of a part of the circle with radius r_1 and angle $(t_{b1}-t_{a1})$.

Similarly, the integration for profiles f_2f_1, f_1a_1, b_1c_1, c_1d_1, and d_1e_1 and lines L_2, L_3, and L_4 can be calculated giving the shaded part areas as the summation of all these integrations.

Since most of the profiles used in the twin screw compressors are circles, straight lines, epicycloids or the envelope curves, it is not difficult to get the solution of the integration functions for these curves. For instance, there are 14 functions in total in the example rotor profiles and most of them can be solved analytically.

The situation when two pairs of points are mating is shown in Figure 5. The shaded area is the uncompressed area. The computation of this area is the same as discussed, however, the two contacting points must be determined first.

After the interlobe contact lines have been completed, the uncompressed area reaches the minimum and the swept area of the grooves becomes maximum. If the rotor continues to rotate, the area between the lobes can not be further invaded by the teeth of the mating rotor and the reduction of the working space in the grooves is caused only by the movement of the interlobe contact lines towards the discharge end.

The subtraction of the uncompressed area from the maximum groove area $f_{01}+f_{02}$ determines the swept area during the compression process and is shown in Figure 6.

The compression volume curve is shown in Figure 7. It is obvious from Figure 7 that the swept area is increasing from

$$\varphi_{10} \longrightarrow \varphi_{1K} = \varphi_{10} + \beta_{01} + \frac{2\pi}{m_1}$$

during which the interlobe contact lines are forming; afterwards the swept area keeps constant from φ_{1k} to t_{1z} and then it becomes smaller while the mating teeth are losing contact from t_{1k} to t_{1z}.

The integration for the lines shown in Figure 2 is the working space volume $v(\varphi_1)$, which at any given turning angle φ is

$$V(\varphi_1) = h \int f_r(\varphi_1)\, d\varphi_1$$

3.4 Unreturn Area

Since most of the modern screw rotors have a large wrap angle there exists a unreturn area during processing, i.e., when the suction process has finished at the inlet end of the rotor. There is still a small part of the female rotor tooth occupied in the male rotor grove and the intake volume for the supply gas becomes smaller then normal. It is necessary to deduct this part of the area from the total. The principle of area computation is the same as before.

4. FLUTE AREA FACTOR AND WRAP ANGLE FACTOR

The discharge volume of the air compressor is calculated by

$$V_d = \eta_v C_n C_\varphi n_1 L_r D_1^2$$

where the c_n and c_φ are the flute area and wrap angle factors respectively. The flute area factor is

$$C_n = m_1 (f_{01} + f_{02}) / D_1^2$$

thus, when the factor of c_n is going to be calculated, the flute area for male and female profile f_{01} and f_{02} have to be computed using the principle of integrating within the closing lines (see Section 3.1).

The angle factor is

$$C_\varphi = 1 - \frac{(\Delta V_{01})_s + (\Delta V_{01})_d}{V_{01} + V_{02}}$$

where v_{01} and v_{02} are the flute volume of the male and female rotor, which is the product of the profile flute area f_{01} or f_{02} and the rotor length l_r. The volumes

$$(\Delta V_{01})_s \quad ; \quad (\Delta V_{01})_d$$

are the occupied volume by the female rotor tooth in one male rotor working space at the suction end and the discharge end respectively, which are calculated using the method described in Section 3.1 When the occupied volume Δv_{01} has the same value at both the inlet end and the outlet end, the most efficient wrap angle factor c_φ is obtained which depends upon the wrap angle of the rotor.

5. LENGTH OF THE SEALING LINES

Since they permit the leakage of the compressed gas, the length of the sealing lines and the blow hole area are important factors effecting the efficiency of twin screw compressors. It is important to attempt to shorten the length of the sealing lines and decrease the area of the blow holes when designing a screw rotor profile set.

When calculating the length of the sealing lines, it is necessary to first determine a set of functions for the male and female profiles in accordance with the coordinate systems, and then to find the rotor lobe surface functions. The general form of such functions is

$$\begin{aligned} x &= x_0(\lambda)\cos\phi \mp y_0(\lambda)\sin\phi \\ y &= \mp x_0(\lambda)\sin\phi + y_0(\lambda)\cos\phi \\ z &= K\phi \end{aligned}$$

where plus and minus signs represent right and left twist directions. Adding the contact condition of the two local surfaces, i.e. at each contact point only sliding movement along the tangent direction is permitted, the function representation of the contact line or sealing line between two surfaces is then obtained,

$$\begin{aligned} x &= x_0(\lambda)\cos\phi \mp y_0(\lambda)\sin\phi \\ y &= \mp x_0(\lambda)\sin\phi + y_0(\lambda)\cos\phi \\ z &= K\phi \\ f&(\lambda, \psi, \phi) = 0 \end{aligned}$$

The length of the sealing line can be computed from integration along the profile. The differential form is

$$ds = \sqrt{(dx)^2 + (dy)^2 + (dz)^2}$$

and the sealing line length is

$$S = \int ds$$

The total length of the interlobe sealing lines is the summation of each section of the contact line of the respective profile. For example, the length of the sealing line for the profile section ef is obtained

$$l_{ef} = \frac{\pi}{180}\,\beta_{01}\sqrt{r_1^2 + \left(\frac{T_1}{2\pi}\right)^2}$$

A more detailed presentation of this analysis can be found in Reference [4].

6. THE BLOW HOLE AREA

The blow hole is generated by the non-symetrical profiles mating, which is widely employed in the modern screw compressors for the reason of the high efficiency. there are two blow holes existing at the ends of the interlobe sealing lines. The shape of the blow holes is an irregular three-d surface and the calculation of the blow hole area is quite difficult. This calculation can be simplified by assuming that the surface is approximated by a plane, which is generally good enough for engineering design. The approximate area of the blow hole as shown in Figure 8 is

$$S_{Hba} \cong \frac{1}{2}\,\overline{Hb}\cdot\overline{ab'}$$

At present the most widespread method of screw rotor manufacture is single index machining (milling or grinding), although there is a certain interest in hobbing, especially for smaller rotors. The current versions of the programs support the single index process, from production of the tool to control of the completed rotor. A similar series of programs for hobbing is in preparation.

In the case of single index milling a number of tool blades of identical shape are fixed to a disk shaped tool body, which is rotated to cut one thread of the rotor at a time. The TOOL program calculates the shape of these blades. The tool axis may be placed in different positions relative to the rotor axis, and the tool blades may be placed at different angles relative to the tool axis. The coordinates of the blades depend on the setup, and some setups will give better cutting conditions and more even wear on the tool than others. In the computation of the tool coordinates the positions of the tool axis and tool blade are given by the user via the keyboard. In addition, a file of 'clearance coordinates' for the rotor is needed as input. This means that the program computes a tool, which theoretically will cut the rotor with nominal clearances applied. Along the entire length of the thread a certain profile point will be cut by a certain point on the tool blade. Coordinate points on the tool will be the points that cut the corresponding coordinate points on the rotor, and they are numbered accordingly. The program reports the cutting angles (front and side rake) at each coordinate point. The user can thus experiment to find a setup with optimal cutting conditions. To improve cutting conditions, one can also make use of two (or more) sets of blades, set alternatingly in the tool body and at different angles, each set cutting part of the profile ('zig-zag tool'). The program is flexible enough to allow the tool blades to be set at any position relative to the tool axis and cut any prescribed part of the complete profile.

Thus the TOOL program computes a tool that theoretically will cut the desired profile. For various reasons that may not be the optimal shape for the tool. For example, the tool will wear with use, and to increase the time between regrinds one may want to add metal to areas of the tool particularly subject to wear. One may also want to compensate for elastic deformations during the cutting process, or other imperfections in the machining process. This could be done by change in the clearance specification, but for several reasons this is inappropriate. The 'clearance coordinates' should describe the shape of the finished rotor, *i.e.*, they are design data. Any changes to the theoretical tool shape needed to cut the rotor should therefore be applied directly to the tool coordinates. Consequently there is a program available to apply modifications to the tool shape which works similarly to the clearance application program.

For many reasons a program for geometric simulation of the cutting process is desirable. For example, it may be used to see the effects on the rotor profile of changing any of the parameters in the machining set up, such as the angle and distance between rotor and tool axes, the location of the tool blade relative to the tool body, *etc.* It can also be used to determine the theoretical shape of a rotor cut with a tool measured in a coordinate measuring machine (CMM) using given settings. Such a program is available. In addition to what has already been mentioned the program produces 'sensitivity coefficients' for all the variables that influence the form of the rotor, *viz.* angle and distance between rotor and tool axes, rotor lead, tool blade rake angles and 'offset' as well as the actual tool coordinates. These coefficients are given for each point of the rotor, and have the following meaning: To see the effect on the rotor profile of *small* changes in all the variables, multiply each sensitivity coefficient by the change in the corresponding variable and add together. The result is the distance the rotor point moves in the direction of the profile normal at the point (presumably the point will also move parallel to the profile, but for small changes this should have very little effect). One use of the sensitivity coefficients is to determine which factors influence rotor form the most in each point; this could be used to determine which points it would be most effective to check, to find out if a certain setting is within acceptable limits.

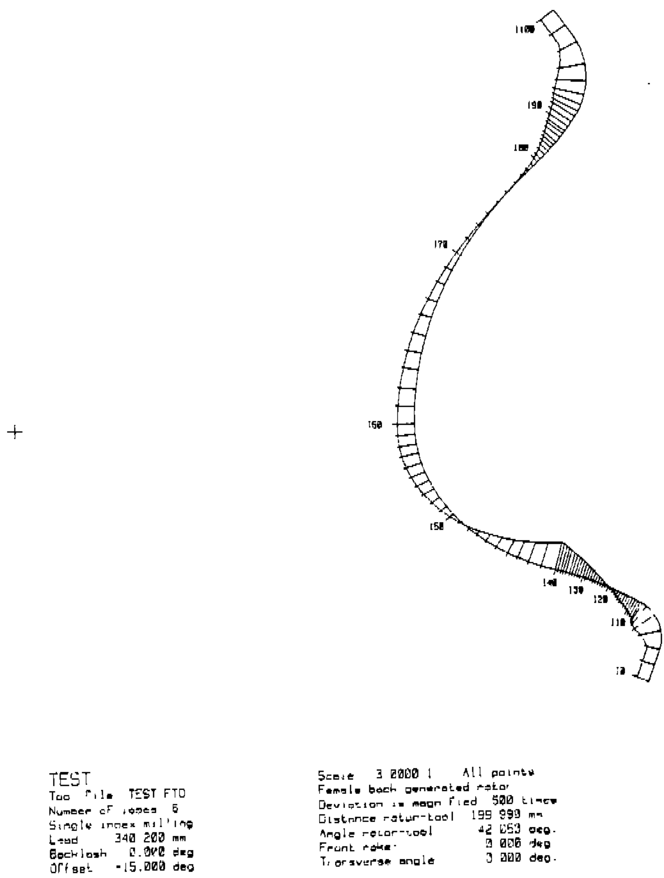

Plot of output from cutter simulation program, showing effect of a slight increase of infeed and cutting angle

The program is also able to use the sensitivity coefficients to determine exactly how much to change each setting to correct a given, measured rotor shape. The measured coordinates are read from a file, and the program then produces a list of changes to be made in settings to get as close as possible to the desired rotor shape. The program then calculates the actual shape of rotor to be expected from the new settings, and the residual errors in the normal direction. The calculation can be done allowing only certain variables to be changed. For example, normally one would not want to change the pitch of the rotor! It might also be of interest to see how close one can get when changing only the machine tool settings without interfering with the tool shape.

In all these calculations only purely geometric factors are taken account of. This means that any elastic deformations in the setup will not be accounted for. This should not matter, however, assuming that profile errors caused by such factors are small. The reason is that the program calculates corrections from a measured profile, so that errors from such sources should be automatically compensated for, as far as is physically possible.

When a rotor is carefully checked in a coordinate measuring machine the output will be a massive amount of raw data. It would normally consist of deviations from the nominal coordinates of the identification points in all the threads and in several cross sections along the rotor. These need to be interpreted to indicate how well a particular rotor corresponds to the theoretical shape. The rotor checking program takes as input a file from the CMM and calculates lead and indexing errors. It draws a diagram to indicate how the rotor size varies along its length, to show errors like tapering or barrel shape, and other diagrams to show the deviation from the theoretical profile in each thread and each cross section.

Routine checking of rotors during manufacturing must of course be done in a less time consuming way than the coordinate measuring machine offers. A simple pairing stand and feeler gauges can be used to give a rough indication of the quality of a rotor pair. To make room for the feeler gauges one would like to set up the pairing stand with an increased center distance, and also always measure with contact between the rotors on the flanks opposite to those between which one is checking ('flip-flop measuring'). There is a program to calculate the permissible gaps at various points along the profile, given the center distance of the pairing stand and the tolerances in intermesh clearances when the rotors are mounted with nominal center distances.

References

1. S. Edström, *A Modern Way to Good Screw Rotors*, Proc. of the 1992 International Compressor Engineering Conference at Purdue.
2. O. Heinemann, A. Koßler and S. Nowotny, *Ein Neuentwickeltes System von Rechenprogrammen zur Erzeugung, Berechnung, Prüfung, Fertigung und Automatischen Messung von Schraubenrotorpaaren für Kältemittelverdichter*, Luft- und Kältetechnik v 23 n 3 (1987), p. 123–131.
3. P. J. Singh and A. D. Onuschak, *A Comprehensive, Computerized Approach to Twin-Screw Rotor Profile Generation and Analysis*, Proc. of the 1984 International Compressor Engineering Conference at Purdue.

REMARKS ON OSCILLATING BEARING LOADS IN TWIN SCREW COMPRESSORS

Glynn Adams and Werner Soedel
Ray W. Herrick Laboratories
School of Mechanical Engineering
Purdue University
West Lafayette, IN 47907

ABSTRACT

Oscillating bearing loads occur in twin screw compressors in the absence of rotor chatter due to several effects. Among these are the time varying moments and forces imparted on each rotor during the compression process. Utilizing assumptions which simplify the rotor profile geometry, a general method for computing the compression loads on each rotor is accomplished. A classical model of tooth interaction between helical gears is then used to obtain the contact forces between the rotors. The subsequent effect of the compression loads on the bearing reactions is presented.

NOMENCLATURE

θ_M	Angle of rotation of the male rotor
A	Projected lobe area
ds	Elemental length along the lobe line
L	Length of compressor rotors along Z axis
τ	Rotor wrap angle
σ	Helix angle
P	Differential pressure across a lobe
P_c	Pressure in a single chamber, specified as a function of θ_M
P_{suct}	Suction pressure
P_{disch}	Discharge pressure
r_i, r_o	Inner and outer radius of lobe
$R_{m,f}$	Pitch radius of the male, female rotor
F_z	Axial component of force on a single lobe due to compression
F_t	Tangential component of force on a single lobe due to compression
F_r	Radial component of force on a single lobe due to compression
F_{tx}, F_{ty}	X and Y components of F_t
F_{rx}, F_{ry}	X and Y components of F_r
$M_{x,y,z}$	Moments acting on a single lobe due to compression
A_r	Chamber area projected onto the radial boundary of the chamber
$C_{x,y,z}$	Contact forces between the mating rotors
$F_{m(x,y,z)}$	Total force loading on the male rotor due to compression
$F_{f(x,y,z)}$	Total force loading on the female rotor due to compression
$M_{m(x,y,z)}$	Total moment loading on the male rotor due to compression
$M_{f(x,y,z)}$	Total moment loading on the female rotor due to compression
$B_{i,(x,y,z)}$	Reaction force at the i^{th} bearing along the $X, Y, or Z$ axis
$L_{m,f}$	Length of male, female rotor shaft
L_i	Distance from plane of rotor contact to the i^{th} bearing
L_i'	Distance from plane of the pressure force resultant to the i^{th} bearing

INTRODUCTION

Previous studies involving the investigation of the noise characteristics of the twin screw compressor [1] have shown that the spectrum of the generated noise includes frequency components which may be attributed to rotor chatter. As part of the ongoing research into rotor chatter, the rotor loading due to the compression process and the associated bearing loads is being investigated. Presented here is a method for determining the bearing loads due to the compression process.

The following assumptions are made in performing this derivation.

- The lobes are assumed to be helical planes. This serves to simplify the complex rotor profile geometry. Due to this assumption, the interlobe seal line is approximated as a straight line parallel with the rotor axis. Although this affects the magnitudes of the computed loads, it does not affect the validity of the approach presented and should predict trends correctly.
- The contact between the rotors is modeled using the theory of involute helical gears. The common normal between the rotors at the point of contact is assumed to be constant. Due to the actual complex profile geometry, this may not be quite true.
- The rotors are assumed to be rigid bodies.

The compression load on each rotor is computed as the summation of the loads on each of it's lobes. This compression load on a single lobe is computed as a function of the male rotor rotation angle, θ_M. The axial, tangential and radial components are computed and resolved into forces and moments in the X,Y and Z directions. Free body diagrams of each rotor are then used to obtain the bearing loads.

AXIAL AND TANGENTIAL LOADS

The following is the derivation of the axial and tangential compression loads on one lobe of a compressor rotor as a function of θ_M. For this derivation, a lobe is defined using the compressor end plates and the seal line as boundaries. Therefore, the lobe develops between the suction plane and the interlobe seal line during suction and decreases between the interlobe seal line and the discharge plane during compression. The load on a single lobe is computed as the differential pressure across the lobe multiplied by the projected area of the lobe. This load is resolved into axial and tangential force components and moments about the X, Y and Z axes.

The differential pressure across a lobe is the difference in the pressures of the chambers which the lobe separates. The chamber pressure as a function of θ_M is used to determine the differential pressure across each lobe.

With the assumptions given previously, a rotor plan is generated which represents an 'unwrapped' version of the rotors, see Figure 1. Utilizing this plan, the elemental projected lobe area is defined. The projected lobe area is computed as

$$dA = dr * ds \tag{1}$$

where

$$ds^2 = (dL)^2 + (r\,d\theta)^2 \tag{2}$$

$$dL = (L/\tau)\,d\theta \tag{3}$$

Therefore

$$ds = \sqrt{(L/\tau)^2 + r^2}\,d\theta \tag{4}$$

This results in an elemental projected lobe area of

$$dA = \sqrt{r^2 + (L/\tau)^2}\,dr\,d\theta \tag{5}$$

The values of the trigonometric functions of the helix angle σ play an important role in evaluating needed integrals. These values are presented for reference

$$\sin\sigma = \frac{r}{\sqrt{r^2 + (L/\tau)^2}} \tag{6}$$

$$\cos\sigma = \frac{L/\tau}{\sqrt{r^2 + (L/\tau)^2}} \tag{7}$$

The load on a single lobe is therefore

$$\int_{\theta_1}^{\theta_2}\int_{r_i}^{r_o} P\sqrt{r^2 + (L/\tau)^2}\,dr\,d\theta \tag{8}$$

with the limits of integration for θ defined by the current value of θ_M.

The axial component of the loading is determined by the helix angle σ. This component is resolved into a force in the Z direction along with moments about the X and Y axes. The axial force is defined as

$$F_z = \int_{\theta_1}^{\theta_2}\int_{r_i}^{r_o} P\sin\sigma\sqrt{r^2 + (L/\tau)^2}\,dr\,d\theta \tag{9}$$

Evaluating the integral gives

$$F_z = (1/2)\,P(r_o^2 - r_i^2)(\theta_2 - \theta_1) \tag{10}$$

An additional component of the axial load is due to the pressure differential across the ends of the rotor shafting, which are exposed to the suction and discharge pressures. This component of the forcing is dependent upon the compressor design. For the case being considered here, this force is computed as $(P_{disch} - P_{suct}) * \pi * r_i^2$. The force is in the positive Z direction and must be added to the value of F_z, computed above.

The moments about the X and Y axes generated by the axial load are computed as follows

$$M_x = \int_{\theta_1}^{\theta_2} \int_{r_i}^{r_o} rP \sin\theta \sin\sigma \sqrt{r^2 + (L/\tau)^2}\, dr\, d\theta \tag{11}$$

$$M_x = -(1/3)\, P(r_o^3 - r_i^3)(\cos\theta_2 - \cos\theta_1) \tag{12}$$

$$M_y = -\int_{\theta_1}^{\theta_2} \int_{r_i}^{r_o} rP \cos\theta \sin\sigma \sqrt{r^2 + (L/\tau)^2}\, dr\, d\theta \tag{13}$$

$$M_y = -(1/3)\, P(r_o^3 - r_i^3)(\sin\theta_2 - \sin\theta_1) \tag{14}$$

Likewise, the tangential component of the pressure load is defined using the helix angle σ. This load is resolved into forces in the X and Y directions along with a moment about the Z axis. The tangential load is defined as

$$F_t = \int_A P \cos\sigma\, dA \tag{15}$$

as shown in Figure 2.

The X component of the tangential load is defined as

$$F_{tx} = \int_{\theta_1}^{\theta_2} \int_{r_i}^{r_o} P \cos\sigma \sin\theta \sqrt{r^2 + (L/\tau)^2}\, dr\, d\theta \tag{16}$$

$$F_{tx} = -P(L/\tau)(r_o - r_i)(\cos\theta_2 - \cos\theta_1) \tag{17}$$

The Y component of the tangential load is defined in the same manner as

$$F_{ty} = -\int_{\theta_1}^{\theta_2} \int_{r_i}^{r_o} P \cos\sigma \cos\theta \sqrt{r^2 + (L/\tau)^2}\, dr\, d\theta \tag{18}$$

$$F_{ty} = -P(L/\tau)(r_o - r_i)(\sin\theta_2 - \sin\theta_1) \tag{19}$$

The moment about the Z axis due to the tangential load is computed as

$$M_z = -\int_{\theta_1}^{\theta_2} \int_{r_i}^{r_o} rP \cos\sigma \sqrt{r^2 + (L/\tau)^2}\, dr\, d\theta \tag{20}$$

$$M_z = -(1/2)\, P(L/\tau)(r_o^2 - r_i^2)(\theta_2 - \theta_1) \tag{21}$$

RADIAL LOADS

The radial load on the rotors due to compression is computed as the product of the chamber pressure and the area of each chamber projected onto the radial surface bounding the chamber. The total radial load on the rotor is the summation of the loads for each chamber.

The X and Y components of the radial load are computed as where $\overline{Hb}$ is the housing crossing line, $\overline{Ha}$ is a screw line created by point e_1, and $\overline{ba}$ is a space curve generated by profile g_2f_2. Therefore, when the coordinates of the points H, a, b, b′ are obtained, the approximate blow hold area can be computed.

7. CONCLUSION

The geometry characteristics discussed above are important for the designer to determine in the development or improvement of the twin screw compressors. One of the more difficult and important calculations is the volume change calculation. An analysis method for this calculation has been presented which possesses both simplicity and accuracy. This method is based on the actual profile functions; most of which can be integrated analytically. The results of this method can be used in the computer simulation and modeling of the twin screw compressors easily.

8. REFERENCE

[1] Deng Dingao and Shu Pengchen, Rotational Compressor, Machinery Industry Publishing House, China.

[2] L. Linder, Screw Compressor, Machinery Industry Publishing House, China

[3] Mitsuru Fujiwara and Katsuhiko Ksuya, "Computer Modeling for Performance Analysis of Rotary Screw Compressor," *Purdue Compressor Technology Conference*, p. 536, 1984.

[4] L. Zhang and J.F. Hamilton, "Development of Sealing Line Calculation in Twin Screw Compressor," *Proc. 3rd International Symposium on Transport Phenomena and Dynamics of Rotating Machinery*, Honolulu, Hawaii, April 1990.

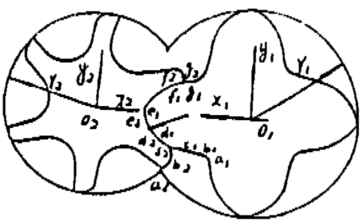

Fig. 1. Rotor Profiles

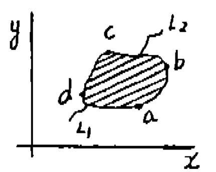

Fig. 2. Area of Closing Lines

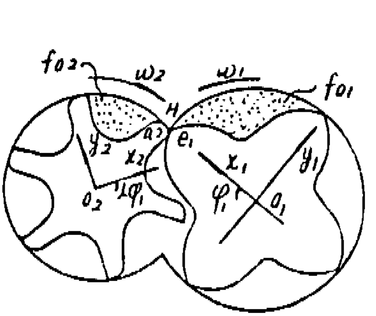

Fig. 3. Flute Area at the Compression Beginning

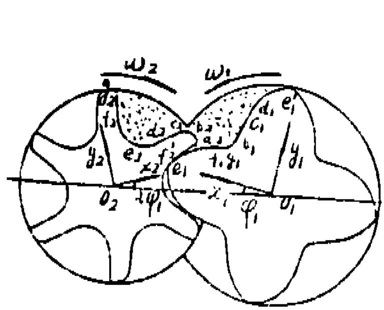

Fig. 4. Flute Area at One Point Mating

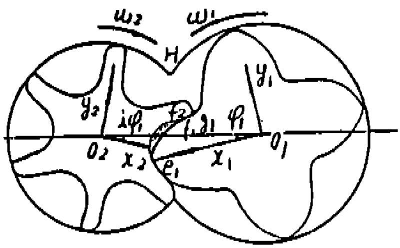

Fig. 5. Flute Area at Two Points Mating

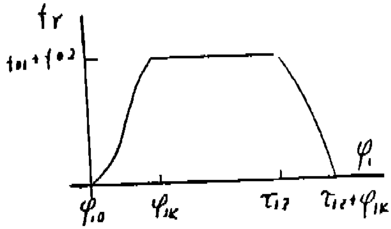

Fig. 6. Flute Area Change along with Rotor Rotation

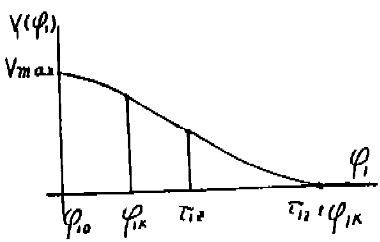

Fig. 7. Volume Change Curve

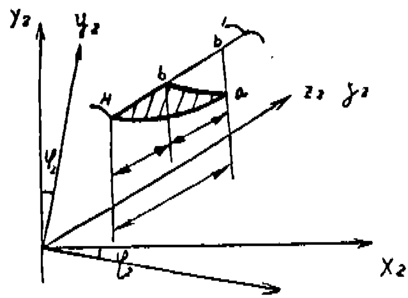

Fig. 8. Blow Hole